The Structure and Orientation of MDBA Self-Assembled Monolayers and Their Interaction with Calcite: A Molecular Dynamics Study

Journal:	*The Journal of Physical Chemistry*
Manuscript ID:	jp-2013-006235.R1
Manuscript Type:	Article
Date Submitted by the Author:	n/a

Complete List of Authors:	Côté, Alexander; University College London, Department of Physics & Astronomy Freeman, Colin; University of Sheffield, Department of Engineering Materials Darkins, Robert; University College London, Department of Physics & Astronomy Duffy, Dorothy; University College London, Department of Physics & Astronomy

The Structure and Orientation of MDBA Self-Assembled Monolayers and Their Interaction with Calcite: A Molecular Dynamics Study.

Alexander S. Côté[1*], Colin L. Freeman[2], Robert Darkins[1] and Dorothy M. Duffy[1]

[1] Department of Physics and Astronomy, University College London, Gower Street, London, WC1E 6BT (UK)

[2] Department of Materials Science and Engineering, University of Sheffield, S1 3JD (UK)

Abstract

We investigate the structure of self-assembled monolayers produced by different mercaptodecyl benzoic acid isomers using molecular dynamics. We examine their interaction with water and calcium carbonate, and analyse the headgroup orientations in each case. We compare our results to experimental findings and propose an explanation for their observed hydrophilicity, as well as for the preferentially oriented growth of calcite on one of the isomers.

Keywords: MDBA; self-assembled monolayers; Molecular Dynamics; calcite; biomineralisation

1. Introduction

Surfaces engineered from self-assembled organic monolayers (SAMs) have been the focus of numerous studies in the past few decades, mainly because of their various applications[1]. One notable example is the crystallisation of calcium carbonate, an extremely common biomineral, where the organised array of headgroups of the SAM not only assist crystallisation, but also exert significant control on the crystal growth and orientation[2]. A popular choice of SAMs for many applications is a ω-terminated alkanethiol, $[X(CH_2)_nS-]$ supported on a gold film,[3-5] where the S end of the chain-like molecule is strongly attached to the Au surface. For long alkane-chains, the molecules pack into an ordered structure and the chains tilt away from the normal direction of the Au surface to lower the energy. The exact packing structure is largely influenced by the choice of headgroup X.

The headgroup is also a factor in the control of mineralisation. It has been shown[3,6] that different headgroups induce different orientations of the formed crystal, sometimes resulting in high energy crystal surfaces. Specifically, COOH-terminated SAMs, give rise to the (01.2), (01.5) or (11.6) nucleation planes, rather than the low energy (10.4) plane. Sulphates (SO_4) and phosphates (PO_4) also induce preferential growth to a small group of crystallographic directions[3]. One also must keep in mind that the SAMs can undergo structural rearrangement during the nucleation process, and the flexibility of the chains, as well as the position of the headgroups, are thought to play a major role[7,8].

Interesting results can be obtained by using aromatic thiols, where the headgroup is a phenyl ring coupled with a functional group. Aromatic thiols have stronger intermolecular interactions

than alkanethiols without the aryl ring, which results in a potentially different packing and, consequently, different surface properties. Also, as electrons are more delocalised in the aryl rings than in the alkane chains, the aromatic thiols have a higher electrical conductivity.9 These properties make them interesting surfaces, but, their formation and packing is still not very well understood.

In a recent study, Lee et al. (2013)[10] used COOH- terminated aromatic thiols as surfaces for calcite growth. They used three subtly different mercaptodecyl benzoic acids (MDBA), the difference being in the position and number of the functional groups attached to the aryl ring. The different isomers, specifically called para- (p-) meta- (m-) and bimeta- (bm-) MDBA, were found to have different properties in solution, and only one of them, the p-MDBA was observed to induce directed crystallisation of calcite, interestingly in the (01.8) orientation. The hydrophilicity of each MDBA SAM was evaluated by static contact angle measurements with water, showing that the surface formed from the m-MDBA SAM is hydrophobic. By using X-ray diffraction (XRD) and Scanning Electron Microscopy (SEM) measurements with different solutions on the SAMs, they were also able to determine the relative angles of the aryl rings with respect to the surface, and show that the p-MDBA undergoes significant reorientation when in contact with water or $CaCO_3$, relative to the other isomers.

In this study we reproduce the above surfaces in silico, using molecular dynamics simulations. We extract the lowest energy configuration of each of the MDBA isomers, and compare our results to experiments. We examine the headgroup orientation of four types of structure, inspired by the experiments. The simulations were carried out both at low temperature and at room temperature. We find that the main reason for the hydrophobic nature of the m-MDBA isomer is

hydrogen bonding between neighbouring carboxyl groups. We compare our results of the headgroup orientation with those of experiment and discuss the trends. Finally we examine the interfacial energy of the (01.8) calcite surface on each isomer and show that this orientation has a stronger interaction with the p-MDBA SAM than the other isomers.

2. Methods

The structures of the para-, meta-, and bimeta-MDBA headgroups are shown in figure 1. The supercell for the simulations was constructed using the cell dimensions of the experimentally measured unit cell of biphenylakanethiol (BP) SAMs with, even-numbered chains, grown on a Au (111) surface[11]. It has been determined[10] that those 'even' BP monomers are close structural analogues of the MDBA monomers, hence their in-plane packing and molecular orientation are expected to be very similar. Our model SAM consists of a supercell periodically repeated in x and y with dimensions x=25.3 Å and y=38 Å, containing 32 MDBA monomers. A vacuum gap of ~65 Å was added in the z-direction, to separate the substrate from the other MDBA layers. Water and/or $CaCO_3$ was then deposited on the surface.

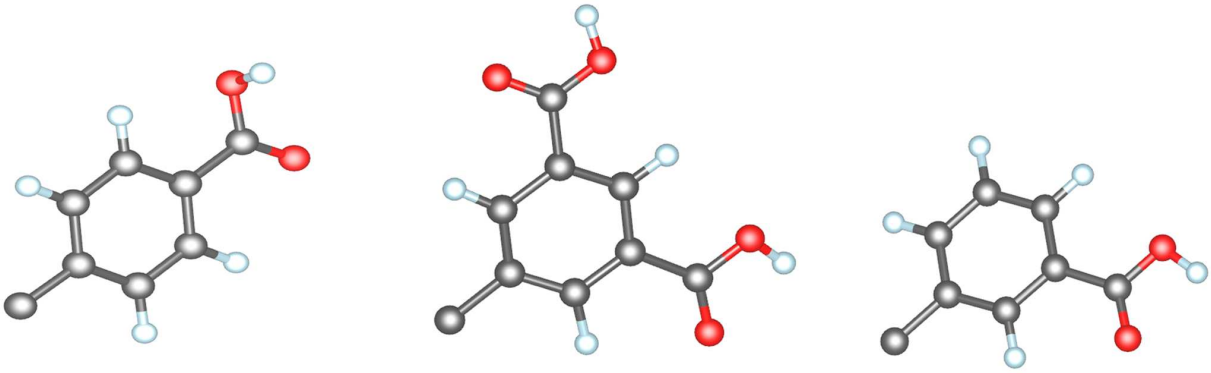

(a) (b) (c)

Figure 1. The structure of (a) p-MDBA (b) bm-MDBA and (c) m-MDBA. Only the aromatic headgroups are shown.

The simulations were carried out using DL_POLY classic v.1.8.[12] The electrostatics were handled by the Ewald summation method and the short-range potentials had a cutoff of 10.1 Å. We used an all-atom potential for the organic molecules, generated with AMBER, and the interactions between the atoms of the monolayer were given by a Lennard-Jones potential. The water was modelled with the TIP3P potential.[13] The organic-calcium interactions were represented by Buckingham potentials. The rest of the organic-inorganic interactions were fitted using the methods described in ref (14), which have already been used successfully in previous studies.[15-17] Calcium carbonate was represented with the force field developed by Pavese et al. [20,21]. The simulation timestep was 0.5 fs in a canonical ensemble using the Nose-Hoover thermostat with a 20 fs relaxation time.

We performed geometry optimisations for the three different isomers, considering a neutral case, where the head groups were fully protonated, and a fully ionised case, where all the H atoms of the COOH groups were removed. The reason for studying both cases is that it is not known experimentally and cannot be easily determined whether the headgroups are protonated or not. The charge on the ionised monolayers was compensated by adding the appropriate number of Ca^{2+} ions. We considered four cases: i) protonated SAMs ii) protonated SAMs with an overlayer of water, iii) ionised SAMs with compensating Ca^{2+} ions and an overlayer of water, and iv) ionised SAM with an overlayer of amorphous calcium carbonate (ACC). The layers of water and ACC (14 Å and 19 Å -thick respectively) were initially placed 2-3 Å above the surface

of the SAM, and relaxed at 300 K onto the SAM, which was kept fixed. After 50 ps the SAM was also allowed to move, until the configurational energy converged. The sulphur atoms were kept fixed to represent the strong bond with the Au substrate, which is not included in the simulation. We found that ~300 ps simulations were sufficient for full convergence. For the geometry optimisation of the SAMs with no overlayers, the temperature was increased in two steps, first to 100 K and then to 300 K; each step was optimised for 50 ps.

In all cases we were able to calculate the average angle of the aryl rings with respect to the surface normal. This corresponds to the total dipole moment vector (TDMV) of the aryl π* -resonance measured experimentally with X-ray absorption spectroscopy (XAS)[10], which describes the functional group orientation of the MDBA monomers (tilt angles). In doing this, we assume that the surface normal coincides with the z-axis of the supercell, i.e. that the surface remains, on average, horizontal.

Finally, in order to investigate the observed preferential growth of calcite in the (01.8) orientation on the p-MDBA surface, a (01.8)-oriented calcite slab of 19 Å thickness was constructed, which was then placed on both the p-MDBA and m-MDBA surfaces. A (10.4)-oriented slab of similar thickness was also placed on the p-MDBA surface for comparison. The (10.4) orientation was chosen for this comparison because it is a low energy surface. The temperature was increased first to 100 K and then to 300 K, and each time the structure was relaxed using the aforementioned settings, for 400 ps. The (01.8) calcite slab has very good epitaxial matching with the COOH headgroups of the monolayer (figure 2). The lattice vectors of the SAM supercells had to be adjusted for each case, but even with the adjustment, they remain within the experimental errors of the BP unit cell on which they are based.[11] This results in a

supercell with 30 monomers, and dimensions x=28.822 Å and y=31.333 Å in the (01.8) case; y increases to 32.196 Å for the (10.4) case. Both neutral and ionised p- and m-MDBA were used to create the SAMs. To model the ionised cases, a layer of charge-neutralising calcium ions were placed on the monolayer surface, and the same number of $CaCO_3$ units were removed from the calcite slab.

The interfacial binding energy of the two isomers with calcite was subsequently calculated, to measure the strength of each interface. This energy effectively represents the cost of cleaving the interface to create two surfaces, in this case separating the calcite slab from the monolayer or, conversely, the adhesion energy for calcite to bind to the monolayer. It can be written as

$$\Gamma = (E_{total} - E_{calcite} - E_{molayer}) / A \quad (1)$$

where $E_{calcite}$ and $E_{monolayer}$ are the energies of the separated calcite and monolayer respectively, and E_{total} is the total energy of the calcite-monolayer system. A is the area of the interface. Even though the above energy Γ is with respect to vacuum, we can still draw a valid conclusion about which isomer presents a preferable substrate for the growth of the deposited calcite surface. According to classical nucleation theory, a lower interfacial energy would result in a lower nucleation barrier and higher nucleation rate.[18,19] The interfacial binding energy is one component of the interfacial energy that is relevant to nucleation.[15] We have not calculated the other components here but we expect the difference between the interfacial binding energies to be the dominant contribution to the difference in nucleation rate.

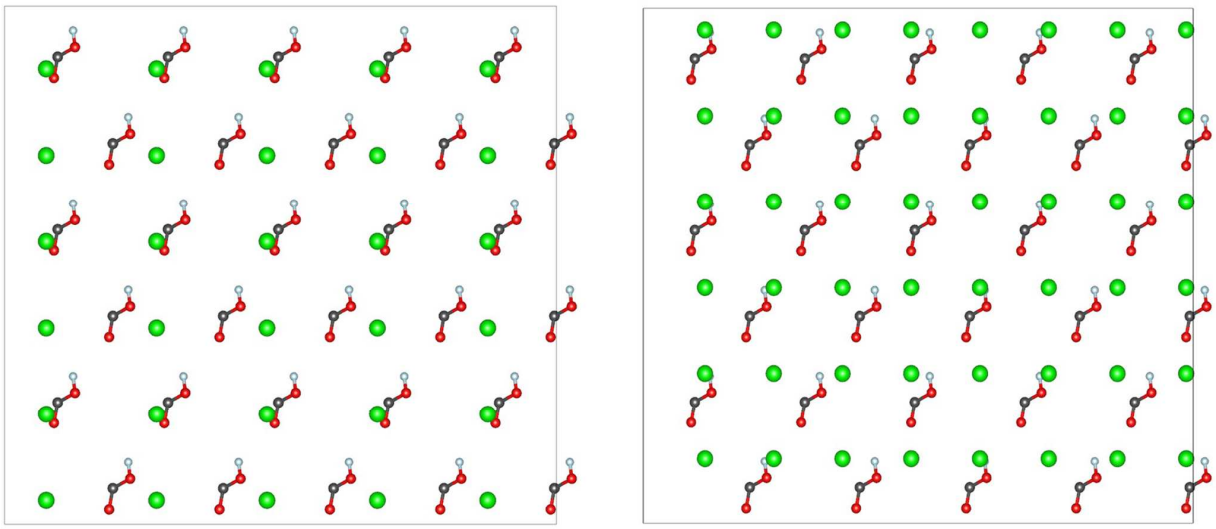

(a) (b)

Figure 2. The starting configurations of (01.8) and (10.4)-oriented calcite on the p-MDBA SAM. Only the lowermost Ca ions (larger green circles) and the carboxyl roots are shown (a) The SAM unit cell contains 30 molecules and there is good epitaxial matching with the (01.8) overlayer of calcite, which has the same number of Ca ions (b) The (10.4) surface contains 48 Ca ions, therefore the epitaxial matching is poorer.

3. Results

3.1 Structure

The decyl chains, about 13 Å long when extended, pack themselves by tilting to a 45° angle so that the thickness of the monolayer, excluding the headgroups, is around 9 Å. This thickness increases to 9.5-10 Å at 300 K. The direction of the chains depends on the isomer, as the interaction of the neighbouring headgroups plays a role in the final packing arrangement.

Figure 3 depicts the three SAMs after optimisation at low temperatures, which allows a clear view of the structures with no temperature-induced defects in the chains. It is interesting to note that the meta and bimeta monolayers show a strong tendency to form hydrogen bonds between the carboxylic acid groups on the phenyl rings, wherever possible, also increasing the structural stability. Especially in the meta- case (figure 3b), all acid groups are hydrogen bonded. Lee et al.[10] have shown that the m- and bm-MDBA SAMs are less flexible than the p-MDBA SAM, because in the first two cases the carboxyl groups are directed into the monolayer, and the headgroups cannot reorient. However, they precluded hydrogen bonds between adjacent monomers whose chains are arranged in a herringbone pattern as are the chains of BP SAMs.[11] We find that a herringbone arrangement has a higher energy, and we show that the hydrogen bonds forming between adjacent monomers are a possible explanation of why the headgroups are not flexible in two of the three isomers.

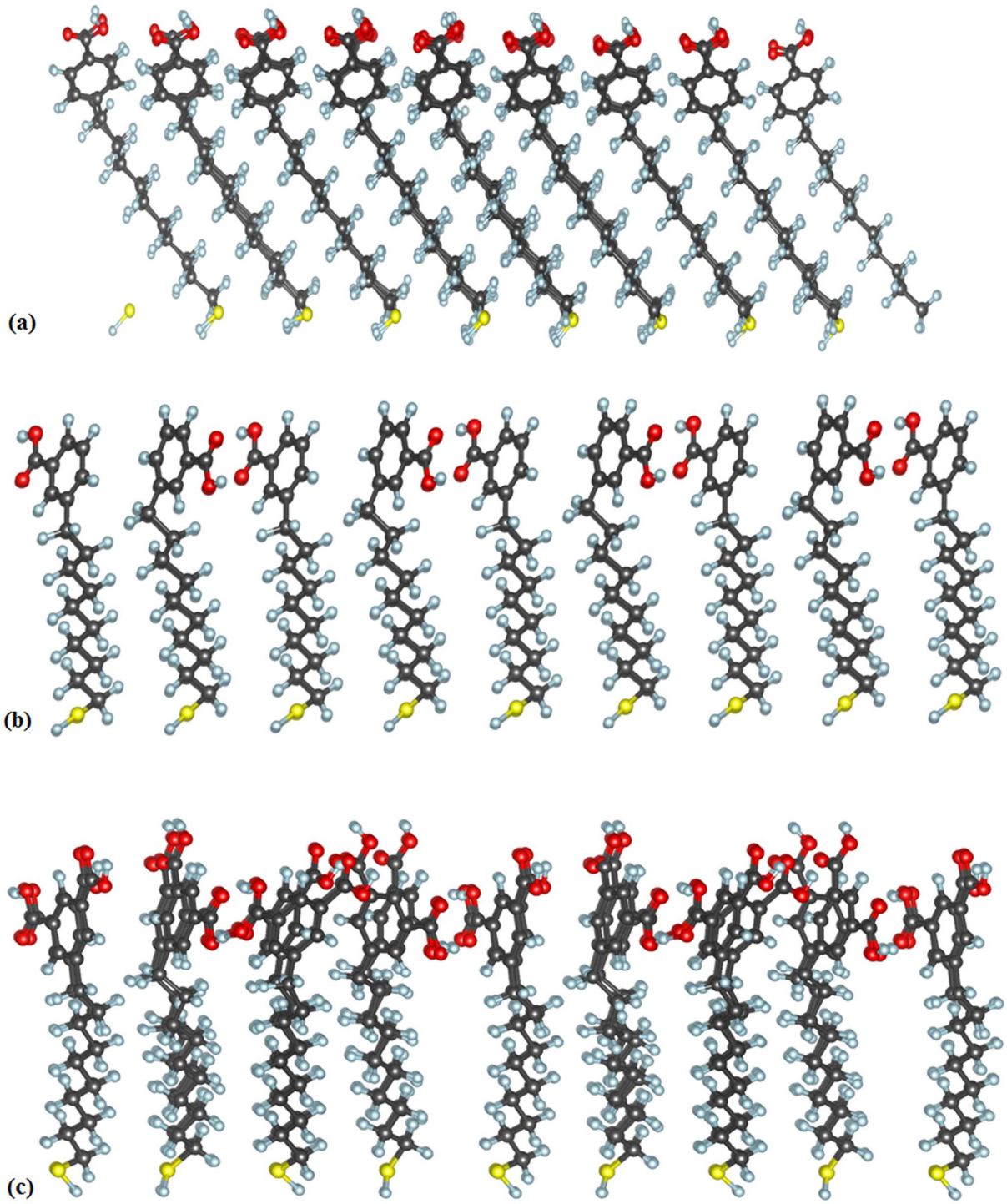

Figure 3. The 3 MDBA isomers used. (a) p-MDBA (b) m-MDBA (c) bm-MDBA. The structures above are equilibrated at low temperatures (30K). Carbon atoms are coloured black, oxygen atoms red, hydrogen atoms light blue and sulphur atoms yellow.

3.2 Solvation

An overlayer of water was added on the MDBA surface at 300K, and snapshots of the 3 protonated SAMs are seen in figure 4. The hydrogen bonded dimerisation of the m-MDBA isomer keeps the carboxyl groups deeper in the surface which results in a reduced interaction with water, in effect making the surface hydrophobic. This is consistent with experimental measurements of wetting[10], where static contact angle measurements showed that m-MDBA displays a far less hydrophilic character than the p- and bm- MDBA isomers, which have accessible carboxyl functional groups.

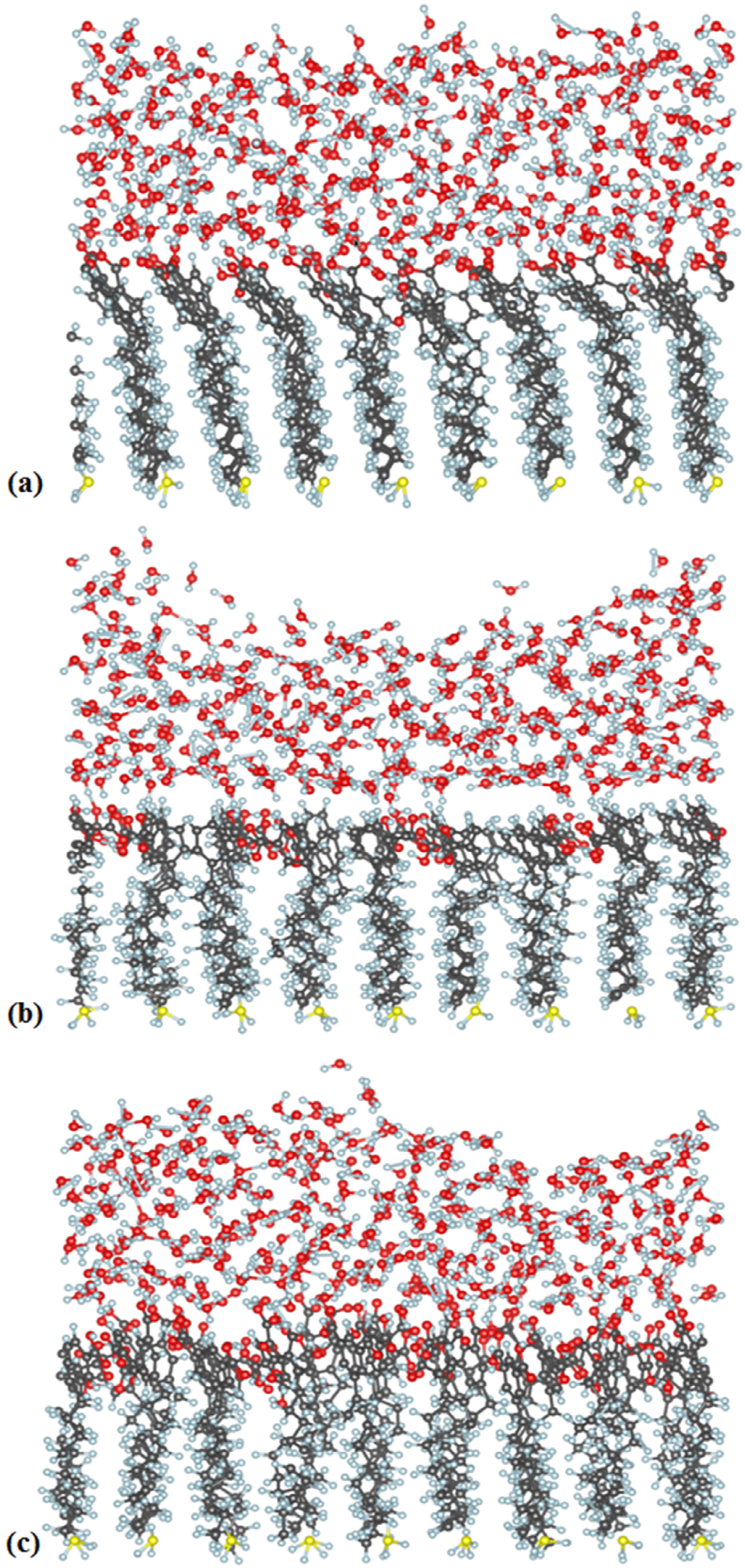
(a)
(b)
(c)

Figure 4. Snapshots of 300 K simulations of neutral solvated SAMs. (a) p-MDBA (b) m-MDBA (c) bm-MDBA. Note the hydrophobic character of the m-MDBA isomer. Carbon atoms are coloured black, oxygen atoms red, hydrogen atoms light blue and sulphur atoms yellow.

The weak interaction with water in the m-MDBA is clear in figure 4b, and in the z-density plots of figure 5. The bm-MDBA, as expected, has a stronger interaction. Its surface is more disturbed than the m-MDBA and the interaction of the water with the free carboxyl groups causes many of the hydrogen bonds to break, however many carboxyl groups remain inaccessible, as seen in figure 4c.

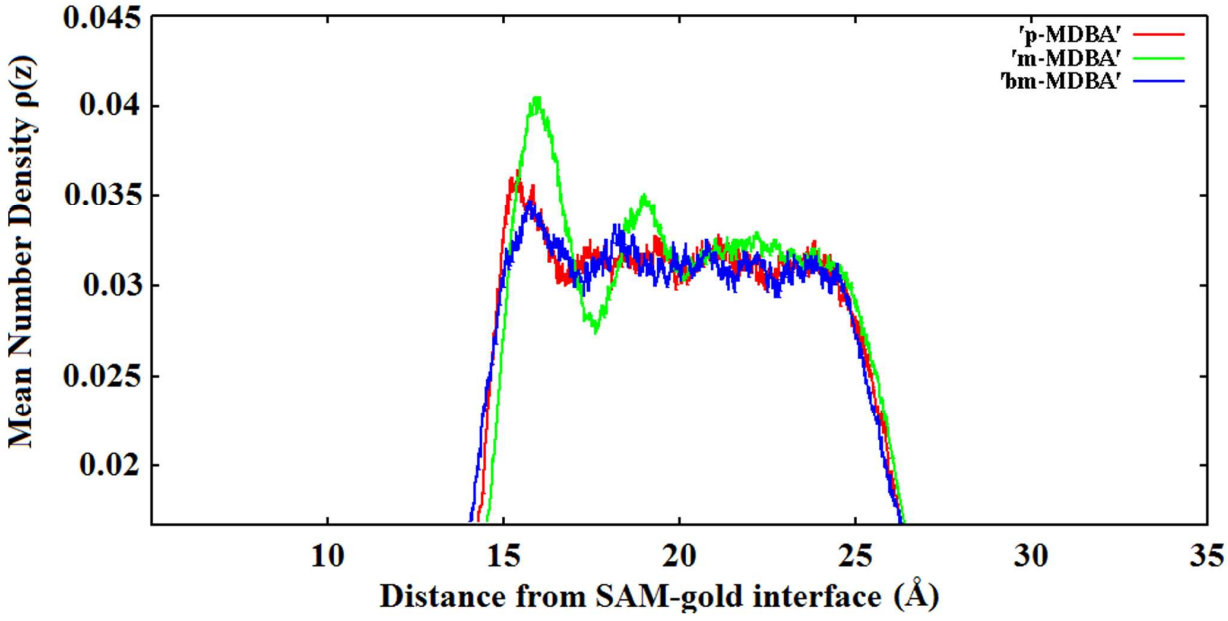

Figure 5. z-density plots of water oxygen atoms on the three protonated SAM surfaces (see figure 4), showing the hydrophobic nature of the m-MDBA monolayer (green line).

If the SAM is ionised, adding water seems to disturb the surface more. The ionised headgroups tend to reorient themselves towards the charge-neutralising calcium ions. The biggest effect was seen in the p-MDBA case, where the carboxyl groups are pointing away from the surface and are closer to the added ions.

3.3 ACC

A ~20 Å-thick periodic slab of ACC was then deposited on the SAM surface. This was done both on a fully protonated and on a fully ionised surface, at 300 K. The aryl rings reorient themselves and the surface order is disturbed considerably in both cases. However, in the case of ACC on the protonated m-MDBA, some of the hydrogen-bonded dimers persisted. Figure 6 shows snapshots of p- and m-MDBA after 200ps. It is clear that the carboxyl groups of the m-MDBA monolayer are buried inside the surface, interacting less with the ACC overlayer than in the p-MDBA case.

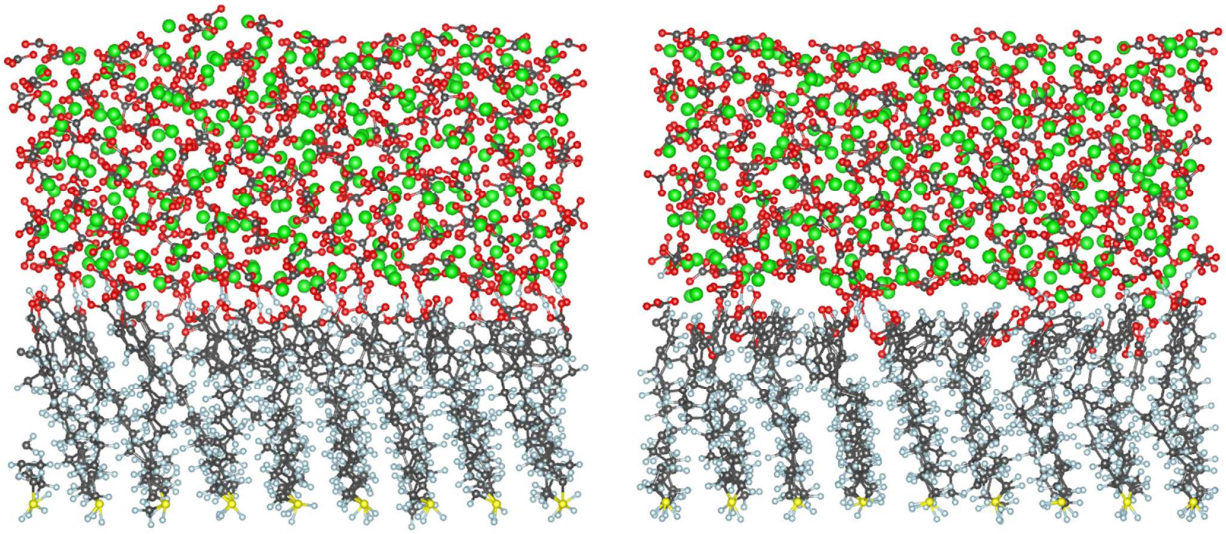

(a) (b)

Figure 6. Snapshots of 300K simulations of protonated (a) p-MDBA and (b) m-MDBA SAMs with an ACC overlayer. The carboxyls in the p-MDBA point away from the surface and interact more with the ACC, forming hydrogen bonds with the carbonates, while in the m-MDBA case the interaction is much less due to the carboxyls pointing inside the surface, and forming dimers with their neighbouring headgroups.

3.4 Headgroup orientation.

We calculated the average aryl ring tilt angles with respect to the surface normal during 300K simulations and the results are summarised in table 1. The values are a time average over 250 ps (neglecting the first 50ps to allow for equilibration). The corresponding experimental results are in brackets.

	TDMV tilt angles				
	As prepared	Solvated	Solvated (ionised)	ACC	ACC (ionised)
p-MDBA	60^{o} (55^{o})	56^{o}	68^{o} (67^{o})	69^{o}	68^{o} (67^{o})
m-MDBA	74^{o} (64^{o})	73^{o}	71^{o} (63^{o})	72^{o}	70^{o} (62^{o})
bm-MDBA	76^{o} (64^{o})	80^{o}	74^{o} (68^{o})	81^{o}	79^{o} (63^{o})

Table 1. TDMV tilt angles for the different SAMs with respect to the Au surface normal. The error on the calculated values is ± 1^{o} and that of the experimental results in brackets is ± 4^{o}

The calculated angles are consistently higher than the experimental angles, but similar trends are observed. In fact, for the p-MDBA case we find very good agreement with experiment. As in the experiments, we can see that for the m-MDBA the exposure to hydrous solution and ACC does not affect the angle, and that the addition of Ca^{2+} bearing solution increases the p-MDBA angles, which in the 'as prepared' and fully protonated solvated case are significantly lower than the isomers that contain hydrogen bonds.

3.5 Calcite

We compared the interfacial binding energies of the p-MDBA and m-MDBA SAMs with an overlayer of the (01.8) surface of calcite, and that of the p-MDBA with a (10.4)-oriented calcite overlayer, on the 30 molecule SAM supercells. The simulations were carried out at 300 K for 300 ps. Tests with a different choice of supercell containing 32 monomers gave higher interfacial binding energies by up to 0.15 J/m^2. This indicates that good epitaxial agreement of calcite on the MDBA SAMs (see figure 2b) accounts for lower interfacial binding energies. The same is evident by the (10.4) case on p-MDBA which has worse epitaxial agreement and a higher interfacial binding energy. In the simulations it was seen, similarly to the ACC case, that the carboxyl groups react with both calcium and carbonate ions, bonding with the calcium ions or, in the non-ionised case, forming hydrogen bonds with the carbonate ions where possible; this behaviour is more pronounced with the p-MDBA (see figure 7). In the m-MDBA case where some hydrogen-bonded dimers still persist, the calcite interacts less with the surface.

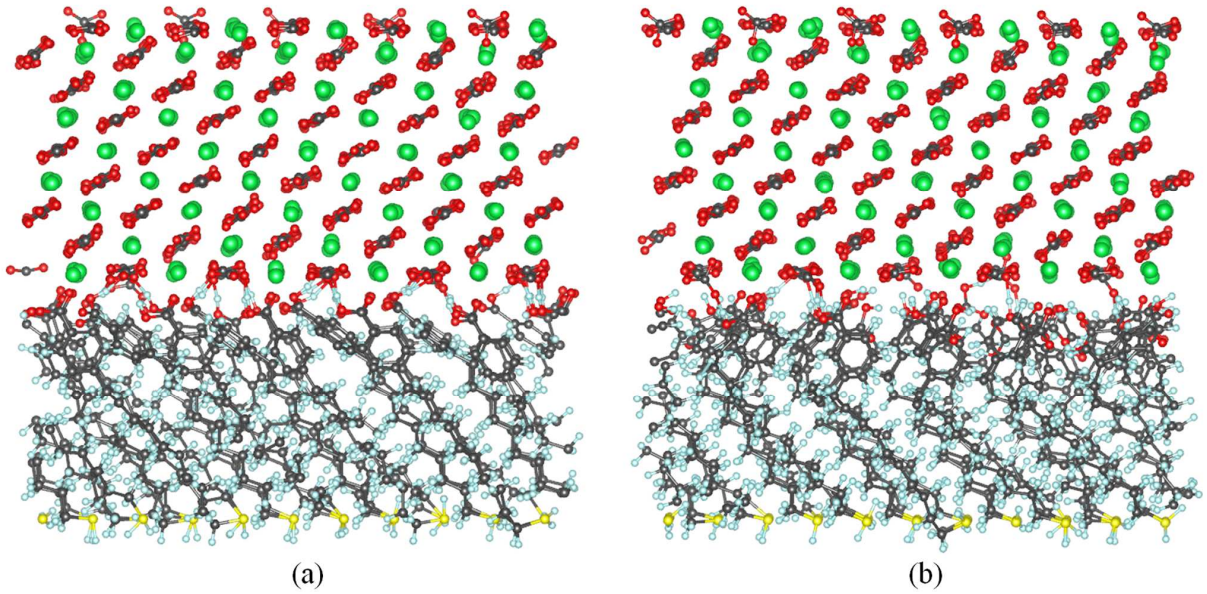

Figure 7. Snapshots of a (01.8)-oriented calcite slab on protonated (a) p-MDBA and (b) m-MDBA at 300 K. The upward orientation of the carboxyl groups of the p-MDBA make the interaction with the calcite overlayer easier than in the m-MDBA case, thus lowering the interfacial binding energy.

The interfacial binding energy of p-MDBA is always lower than the m-MDBA, regardless of epitaxial matching, as shown in table 2. We conclude that, in accordance to experimental findings[10], oriented crystallisation of (01.8) calcite is more favourable on the p-MDBA surface, even though the (10.4) surface has very similar energy. The (01.8) surface was also shown by Darkins et al.[22] to crystallise from an amorphous state at a considerably faster rate than most of the other orientations, including (10.4), a fact that might contribute to the predominance of that particular surface on the p-MDBA SAM.

	Interfacial binding energy (J/m^2)	
	Protonated	**Ionised**
p-MDBA (01.8)	-0.90	-1.29
m-MDBA (01.8)	-0.62	-1.07
p-MDBA (10.4)	-0.88	-1.23

Table 2. Calculated interfacial binding energies of calcite and p/m-MDBA. The (01.8) surface on the p-MDBA isomer is favoured

4. Conclusions

We have performed a series of simulations for three MDBA SAM isomers in different ionisation states. We examined the structural changes of the monolayers upon addition of water and ACC, and compared our results with experimental findings. We established that the m-MDBA isomer forms hydrogen bonds when protonated, which keeps the carboxyl groups buried in the surface and makes it hydrophobic, and less reactive with ACC. Our results of the aryl ring tilt angles show a similar trend with experiment, albeit they have consistently higher values. This discrepancy may be attributed to the existence of lower energy structures, or the lack of sufficient accuracy in the interaction potentials used. We also assumed full ionisation of the carboxyl groups with the Ca^{2+} solution which may not be the case, especially with the hydrogen bonded SAMs. However the similarities in the trends observed by modelling and experiment are encouraging.

Interfacial binding energies were calculated for an overlayer of calcite in the (01.8) and the (10.4) orientations, and we found that p-MDBA is the isomer that most favours the (01.8) orientation, in agreement with experiment. We have shown that by individually analysing the effects of ionisation, headgroup orientation and epitaxial matching, we can explain experimental observations and offer valuable insight into the crystallisation of calcite on different organic surfaces.

Corresponding Author

* Email: a.cote@ucl.ac.uk

Notes

The authors declare no competing financial interest.

Acknowledgements

The authors acknowledge the use of the UCL *Legion* High Performance Computing Facility, and associated support services, in the completion of this work. The work was supported by the Engineering and Physical Sciences Research Council grant number EP/I001514/1. This Programme Grant funds the Materials Interface with Biology (MIB) consortium. RD acknowledges funding from EPSRC under the Molecular Modelling and Materials Science Industrial Doctorate Centre and from Pacific Northwestern National Laboratory

References

(1) Ulman, A. *An Introduction to Ultrathin Organic Films*; Academic Press: Boston, **1991**

(2) Freeman, C. L.; Harding, J. H.; Duffy, D. M. Simulations of Calcite Crystallization on Self-Assembled Monolayers. *Langmuir* **2008**, *24*, 9607-9615

(3) Aizenberg, J.; Black, A. J.; Whitesides, G. M. Oriented Growth of Calcite Controlled by Self-Assembled Monolayers of Functionalized Alkanethiols Supported on Gold and Silver. *J. Am. Chem. Soc.* **1999**, *121*, 4500-4509

(4) Laibinis, P. E.; Whitesides, G. M. Ω-Terminated Alkanethiolate Monolayers on Surfaces of Copper, Silver, and Gold Have Similar Wettabilities. *J. Am. Chem. Soc.* **1992**, *114*, 1990-1995

(5) Nuzzo, R. G.; Dubois, L. H.; Allara, D. L. Fundamental Studies of Microscopic Wetting on Organic Surfaces. 1. Formation and Structural Characterization of a Self-Consistent Series of Polyfunctional Organic Monolayers. *J. Am. Chem. Soc.* **1990**, *112*, 558-569

(6) Han Y-J; Aizenberg, J. Face-Selective Nucleation of Calcite on Self-Assembled Monolayers of Alkanethiols: Effect of the Parity of the Alkyl Chain. *Angew Chem Int Ed*. **2003,** *42*, 3668-3670

(7) Duffy DM and Harding, J., Simulation of Organic Monolayers as Templates for the Nucleation of Calcite Crystals. *Langmuir* **2004**, *20*, 7630-7636

(8) Quigley, D.; Rodger, P. M.; Freeman, C. L.; Harding, J. H.; Duffy, D. M. Metadynamics Simulations of Calcite Crystallization on Self-Assembled Monolayers. *J. Chem. Phys*. **2009**, *131*, 094703

(9) Jin, Q.; Rodriguez, J. A.; Li, C. Z.; Darici, Y.; Tao, N. J. Self-Assembly of Aromatic Thiols on Au(111). *Surface Science* **1999**, *425*, 101-111

(10) Lee, J.R.I.; Han, T.Y-J.; Willey, T.M; Nielsen, M.H.; Klivansky, L.M.; Liu, Y.; Chung, S-W.; Terminello, L.J.; van Buuren, T.; De Yoreo, J.J. Cooperative Reorganization of Mineral and Template during Directed Nucleation of Calcium Carbonate. *J Phys. Chem. C*, **2013**, submitted.

(11) Cyganik, P.; Buck, M.; Azzam, W.; Wöll, C. Self-Assembled Monolayers of Ω-Biphenylalkanethiols on Au (111): Influence of Spacer Chain on Molecular Packing. *J. Phys. Chem. B* **2004**, *108*, 4989-4996

(12) Smith, W.; Forester, T. R. DL_POLY 2.0: A General-Purpose Parallel Molecular Dynamics Simulation Package *J. Mol. Graph. Model.* **1996**, *14*, 136-141

(13) Jorgensen, W. L.; Chandrasekhar, J.; Madura, J. D.; Impey, R. W.; Klein, M. L. Comparison of Simple Potential Functions for Simulating Liquid Water. *J. Chem. Phys.* **1983**, *79*, 926-936.

(14) Freeman, C. L.; Harding, J. H.; Cooke, D. J.; Elliott, J. A.; Lardge, J. S.; Duffy, D. M. New Forcefields for Modeling Biomineralization Processes. *J. Phys. Chem. C* **2007**, *111*, 11943-11951.

(15) Duffy, D. M.; Travaille, A. M.; van Kempen, H.; Harding, J. H. Effect of Bicarbonate Ions on the Crystallization of Calcite on Self-Assembled Monolayers. *J. Phys. Chem. B* **2005**, *109*, 5713-5718

(16) Duffy D.M; Harding, J.H. The Crystallisation of Calcite Clusters on Self-Assembled Monolayers. *Surf. Sci.* **2005**, *595*, 151-156

(17) Duffy D.M; Harding, J.H. Modelling the Interfaces between Calcite Crystals and Langmuir Monolayers. *J. Mater. Chem.* **2002**, *12*, 3419-3425

(18) Hu, Q.; Nielsen, M. H.; Freeman, C. L.; Hamm, L. M.; Tao, J.; Lee, J. R. I.; Han, T. Y. J.; Harding, J. H.; Dove, P. M.; De Yoreo, J. J. The Thermodynamics of Calcite

Nucleation at Organic Interfaces: Classical Vs. Non-Classical Pathways. *Faraday Discuss.* **2012**, *159*, 509-523

(19) Travaille, A. M.; Steijven, E. G. A.; Meekes, H.; van Kempen, H. Thermodynamics of Epitaxial Calcite Nucleation on Self-Assembled Monolayers. *J. Phys. Chem. B* **2005**, *109*, 5618-5626

(20) Pavese, A.; Catti, M.; Price, G. D.; Jackson, R. Interatomic Potentials for $CaCO_3$ Polymorphs (Calcite and Aragonite), Fitted to Elastic and Vibrational Data. *Physics and Chemistry of Minerals* **1992**, *19*, 80-87

(21) Pavese, A.; Catti, M.; Parker, S. C.; Wall, A. Modelling of the Thermal Dependence of Structural and Elastic Properties of Calcite, $CaCO_3$. *Physics and Chemistry of Minerals* **1996**, *23*, 89-93

(22) Darkins, R.; Côté, A.S.; Duffy, D.M. Crystallisation Rates of Calcite from an Amorphous Precursor in Confinement. *J. Crys. Growth*, **2013**, *367*, 110-114

Table of Contents figure